RSC Advances

ROYAL SOCIETY OF CHEMISTRY

www.rsc.org/advances

RSC Advnces

ARTICLE

Facile synthesis of cysteine-functionalized graphene quantum dots for a fluorescence probe for mercury ions

Tran Van Tam, Soon Ho Hong* and Won Mook Choi*

Cystenine-functionalized graphene quantum dots (cys-GQDs) were synthesized by a simple and facile method, which involves a chemical bond formation between L-cysteine and graphene quantum dots (GQDs) prepared by the carbonization of citric acid. The obtained cys-GQDs show a strong green fluorescence and a uniform lateral size distribution with high crystallinity. The cys-GQDs are further demonstrated as highly sensitive and selective fluorescence probes for Hg^{2+}. In the Hg^{2+} detection process, the cys-GQDs shows significant fluorescence quenching through a charge transfer process within the complex of cys-GQDs and Hg^{2+}.

Introduction

Graphene, a one-atom-thick planar sheet of sp^2-hybridized carbon atoms packed in a honeycomb lattice, is now a promising material for various applications.[1-4] Among graphene-based materials, graphene quantum dots (GQDs), the zero-dimensional form of graphene with diameters below 100 nm, have attracted growing research interest for their tunable electronic and opto-electronic properties, which are directly associated with quantum confinement and chemical functionalization. In comparison with the traditional semiconductor quantum dots, GQDs possesses excellent characteristics such as high photoluminescent activity, stable fluorescence without photobleaching, biocompatibility, and low toxicity.[5-7] Many efforts have been made in their preparation and tremendous synthetic methods developed. Generally, GQDs can be produced using top-down or bottom-up approaches. The former approach involves the decomposition of carbon-based materials, including carbon nanotube, carbon fiber and graphene oxide, using physical or chemical treatments.[8-12] The time-consuming oxidative-cutting method is typically used to synthesize GQDs, which are of non-uniform size and low production yield. By contrast, the bottom-up strategy has been developed using small cyclic molecules by the hydrothermal process or high-temperature pyrolysis with easy control of lateral size.[13,14] This approach, however, results in poor quality GQDs and a complicated synthesis process. The covalent functionalization of GQDs is a strategy to tailor their electronic, chemical, physiochemical and photophysical properties. Up to now, few studies have focused on covalent functionalization of GQDs, and the

reported processes require many complicated purification steps.[15, 16] In this regard, the development of the simple functionalization of GQDs remains highly desirable.

Due to strong toxicity and bioaccumulation of heavy metal ions, it is important to develop novel and rapid detection methods with high sensitivity for their detection. Among the various sensing methods, fluorescence sensing approaches have been utilized for the detection of metals because of their excellent sensitivity, fast response, ease of operation and ability to detect in a non-destructive manner. Semiconductor quantum dots (QDs) are widely used for the fluorescence probe owing to their high quantum yield, wide light-absorption band, and size-tunable emission profiles.[17,18] As a new class of sensor materials, fluorescence probes of GQDs have been reported on in various studies, due to their excellent optical properties, biocompatibility, and good solubility in polar and non-polar solvents.[19] These characteristics make GQDs-based advanced fluorescent sensors potentially promising for highly sensitive and selective detection of heavy metal ions. In this work we report a low cost, green and simple strategy for the synthesis of cysteine functionalized GQDs (cys-GQDs). Using the method proposed here, cys-GQDs are synthesized with a uniform lateral size distribution and a strong green photoluminescence with a high quantum yield. The obtained cys-GQDs are employed for the specific detection of Hg^{2+}, which exhibits a highly sensitive and selective fluorescent sensor for Hg^{2+} detection even at low concentrations. Moreover, we have successfully demonstrated the applicability of cys-GQDs for Hg^2 detection in a real water sample.

Experimental

Synthesis of cys-GQDs

The synthesis of GQDs was prepared by the method described in our previous report.[20] In a typical experiment, citric acid (CA, 3.2 g) and distilled water (80 ml) were mixed by constant

School of Chemical Engineering, University of Ulsan, 93 Daehak-ro Nam-gu, Ulsan 680-749, Republic of Korea. E-mail: shhong@ulsan.ac.kr (S.H. Hong) and wmchoi98@ulsan.ac.kr (W.M. Choi).
† Electronic supplementary information (ESI) available. See DOI:

RSC Advances Accepted Manuscript

stirring at room temperature for 30 minutes, followed by sonication for 30 minutes to form a clear solution. After the solution was adjusted to pH 10 by using potassium hydroxide, it was transferred into a 150 ml Teflon-lined stainless autoclave. The autoclave was sealed and heated to 160°C in an oven for 4 hours, and the resultant yellow solution was cooled to room temperature. L-cysteine was added into the yellow solution with constant stirring for 30 min, and the mixture was refluxed at 80°C for 24 hours. Subsequently, the mixture solution was dialyzed using a dialysis bag (3,000 Da, Spectrum Lab. Inc) for two days to remove potassium hydroxide and small impurities. Finally, a light yellow solution of cys-GQDs was obtained. For the characterizations, the samples of cys-GQDs was prepared by adding 0.8 wt% of L-cysteine in the functionalization process.

Characterizations

The nanostructures of cys-GQDs were examined with a high resolution transmission electron microscope (HR-TEM, JEM-2100F, JEOL) and atomic force microscopy (AFM; Veeco, Dimension 3100) in tapping mode. X-ray photoelectron spectroscopy (XPS; Thermo Fisher) measurements were performed using monochromatic AlKα radiation (hv = 1486.6 eV). Proton nuclear magnetic resonance (1H-NMR) spectra and UV-visible absorption spectra were recorded with a Bruker Avance 400 spectrometer (400.13 MHz) and Specord 210 UV-vis spectrophotometer, respectively. Raman spectroscopy (DXR Raman spectrometer, Thermo Scientific) was acquired from 1,000 to 2,000 cm^{-1} at room temperature with a 532 nm excitation source, and Fourier transform infrared (FT-IR, Nicolet IR 200 spectrometer, Thermo Scientific) spectra were measured to verify the functional groups. Fluorescence spectroscopy (Cary Eclipse Fluorescence Spectrophotometer, Agilent) and time-resolved fluorescence (Spex Fluorolog-3, Horiaba) were performed at room temperature. For the Hg^{2+} detection experiments, 1 ml of cys-GQDs solution (0.03 mg/ml) was prepared and mixed with 1 ml solutions of the different Hg^{2+} concentrations. The mixture was left for 5 minutes at room temperature, followed by fluorescence spectra measurements with the excitation wavelength of 420 nm. Furthermore, detection experiments of various metal ions were performed using various metal ion sources, such as Hg(NO$_3$)$_2$, Pb(NO$_3$)$_2$, Cd(NO$_3$)$_2$. 4H$_2$O, NaCl, KCl, Fe(NO$_3$)$_3$.9H$_2$O, Mn(NO$_3$)$_2$.xH$_2$O, Cr(NO$_3$)$_3$.9H$_2$O, Zn(NO$_3$)$_2$, LiNO$_3$, Cu(NO$_3$)$_2$, and AgNO$_3$. A 1 ml metal ion solution was added to 1.0 ml of cys-GQDs solution (0.03 mg/ml) with retention for 5 minutes, and then the fluorescence spectra were recorded with the excitation wavelength of 420 nm. The fluorescence quenching efficiency of cys-GQDs can be well described by the following Stern-Volmer equation:

$$\frac{F_0}{F} - 1 = K_{sv}[Q]$$

where F_0 and F are the fluorescence intensities of cys-GQDs in the absence and presence of metal ions, K_{SV} is the Stern-

Volmer quenching constant and $[Q]$ is the concentration of metal ions.
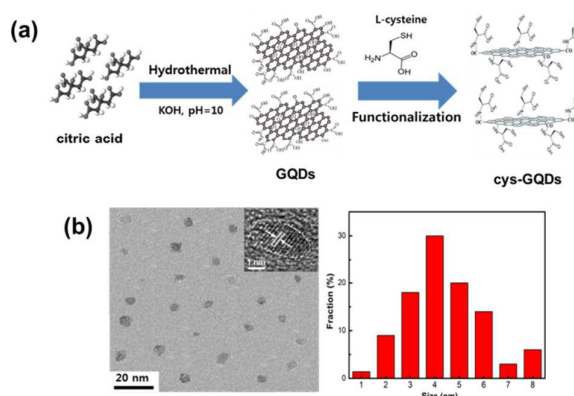
Fig. 1 (a) Schematic illustration of the synthesis of cys-GQDs. (b) TEM images of the synthesized cys-GQDs and their size distribution.
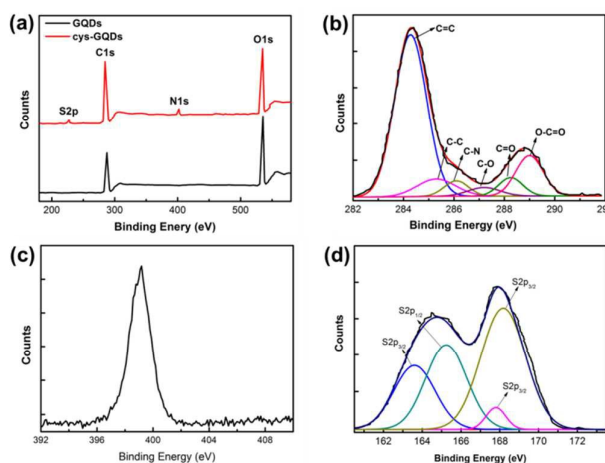
Fig. 2 (a) XPS survey scan of as-prepared GQDs and cys-GQDs. (b) C1s, (c) N1s and (d) S2p core-level XPS spectra of cys–GQDs.

Results and discussion

Fig. 1a shows a schematic of the preparation of cys-GQDs comprising the synthesis of GQDs using CA and the functionalization of GQDs with L-cysteine as precursors. First, CA is carbonized and converted into small graphitic dots by the hydrothermal process at high temperature. During the hydrothermal process, the graphitic dots undergo diffusion and condensation to form crystalline GQDs, containing oxygen functional groups (carboxylic and epoxide) at the basal plane and the edge. Then, the synthesized GQDs are simultaneously functionalized using L-cysteine in the base environment through the amidation reaction which occurs between NH$_2$ of L-cysteine and the oxygen functionalities of GQDs.[21] Therefore, L-cysteine molecules are stably anchored on GQDs surface due to these strong chemical bonds. The TEM image of the prepared cys-GQDs in Fig. 1b reveals a fairly uniform size distribution of samples with an average lateral diameter of 3.8

nm. In addition, the graphitic lattice of GQDs can be clearly observed in the HR-TEM image (the inset of Fig. 1b). The observed lattice spacing of 0.25 nm corresponds to the hexagonal lattice plane spacing of $d_{1120,}$[9] indicating that the synthesized cys-GQDs are of high crystallinity. The AFM results (Fig. S1) reveal that the average height of the cys-GQDs is about 1.25 nm, suggesting that they are mostly single-layered.[10,22]

XPS measurements were performed to investigate the atomic composition and chemical bonding of the cys-GQDs and presented in Fig. 2. While the wide scan survey XPS spectrum of pristine GQDs shows only two peaks, of C1s at 284 eV and O1s at 532 eV, the wide scan spectrum of cys-GQDs exhibits two new peaks, of N1s and S2p at 399.8 and 167 eV, respectively, as evidence of the functionalization of GQDs by L-cysteine (Fig. 2a). The strong C1s peak corresponding to sp^2 carbon indicates that the conjugated bonds in graphene lattice are retained after the functionalization. Compared to the pristine GQDs, the O1s peak intensity of the cys-GQDs decreases, which indicates that the reduction of oxygen functionalities in GQDs occurs by the functionalization by L-cysteine. The high resolution C1s spectrum of cys-GQDs (Fig. 2b) is deconvoluted into six components, corresponding to C=C (284.5 eV), sp^3 carbon (285.4 eV), C-N (286.3 eV), C-S/C-O (287.6 eV), C=O (288.2 eV) and O-C=O (289 eV), whereas the nitrogen functional peak is not observed for the pristine GQDs (Fig. S2). However, the C-N bond peak is observed due to the amine groups of L-cysteine on the cys-GQDs surface, confirming the amidation reaction between L-cysteine and GQDs as described above. The relative content of the amide groups of cys-GQDs is calculated by integrating the fitting curve area of C1s XPS, which is determined to be approximately 16%. The high resolution N1s spectrum of cys-GQDs (Fig. 2c) shows a clear peak of the pyrrolic N (C-NH-C) at 399.4 eV. The high resolution S2p spectrum (Fig. 2d) shows an $S2p_{3/2}$ peak at 163.3 eV, assigned to the thiol group (S-H) of L-cysteine molecules. The other peaks at 165.12, 167.78 and 168.19 eV may be attributed to the phenomenon of spin orbit separation. These results suggest that the cys-GQDs are synthesized by the amidation reaction between the amine groups of L-cysteine and the carboxylic groups of GQDs. The FT-IR and Raman characterization of pristine GQDs and cys-GQDs are further performed to confirm the synthesis of cys-GQDs. In the FT-IR spectra (Fig. S3a), the pristine GQDs have a broad O-H stretching peak at 3400 cm^{-1}, a C=C stretching peak at 1623 cm^{-1}, and a C-O stretching peak in the carboxylic groups at 1398 cm^{-1}. The cys-GQDs exhibit new absorption peaks at 3340, 2870, 1725, and 1250 cm^{-1}, corresponding to N-H bending, S-H stretching peak, C-N stretching vibration, and C=O absorption, whose functional groups are formed after the functionalization. These results clearly confirm that L-cysteine is covalently bonded to the surface of GQDs, which is consistent with the XPS results. Raman spectra were measured to further confirm the quality of the prepared cys-GQDs. Raman spectra of pristine GQDs and cys-GQDs (Fig. S3b) show that the pristine GQDs and the cys-GQDs both have two dominant peaks, which are a G peak at around 1600 cm^{-1},

related to the in-plane vibration of the sp^2 carbon lattice, and a D peak at around 1360 cm^{-1}, related to the presence of sp^3 structural defects. Compared to the pristine GQDs, the cys-GQDs exhibit significant red shifts of both G and D peaks. The G and D peaks shift from 1607 to 1584 cm^{-1} and from 1355 to 1342 cm^{-1}, respectively. The red shift of Raman spectra for the cys-GQDs could be explained by the functionalization of L-cysteine molecules on the surface of GQDs. [21,23,24] Furthermore, the ratio of the intensities of the D and G peaks (I_G/I_D) is 1.09 for the pristine GQDs and 1.06 for the cys-GQDs, showing that both the pristine GQDs and the cys-GQDs are highly crystalline.
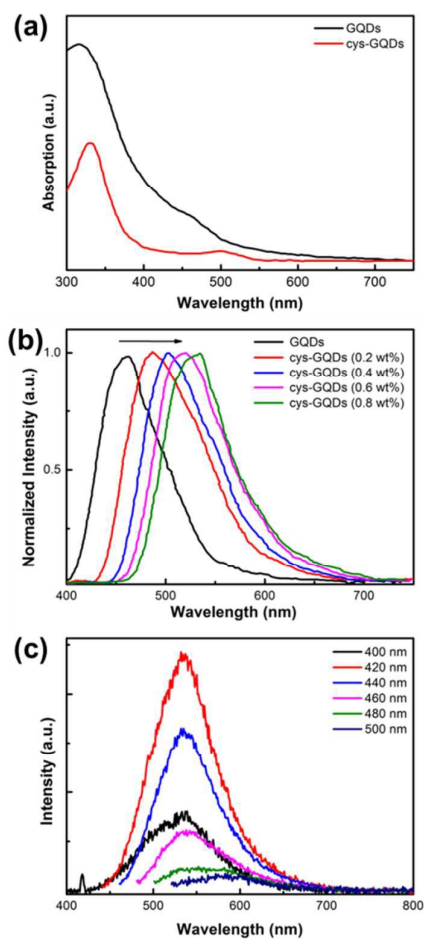
Fig. 3 (a) UV-vis adsorption of GQDs and cys-GQDs. (b) Photoluminescence spectra of cys-GQDs with various amounts of L-cysteine. (c) The fluorescence spectra of cyst-GQDs at different excitation wavelengths ranging from 400 nm to 500 nm.

To analyze the optical properties of cys-GQDs, we performed UV-Vis absorption and PL analysis of the prepared cys-GQDs aqueous solution. The UV-Vis absorption spectrum of the pristine GQDs (Fig. 3a) exhibits a strong peak at 321 nm and a shoulder at 452 nm, corresponding to the electron transitions from π to π* of C=C and C=O bonds. However, the UV-Vis spectrum of cys-GQDs shows a clear shift of the two absorption peaks to 331 and 503 nm after the

functionalization of GQDs with L-cysteine.[25] The PL emission spectra of the obtained cys-GQDs with the various concentrations of L-cysteine when excited at 365 nm are presented in Fig. 3b. However, the emission peak of the pristine GQDs is observed at 460 nm, the emission peak of the cys-GQDs demonstrates a red-shifted with increases in the L-cysteine concentration. The wavelength at the emission peak is shifted from 485 to 532 nm when the concentration of L-cysteine increases from 0.2 to 0.8 wt%, demonstrating the tunable fluorescence of cys-GQDs. In addition, the strong orbital interaction between the amine group and the π-conjugated system of functionalized GQDs can lift the degenerate HOMO orbitals to higher energy, which could explain the red shift of PL spectra.[26] Fig. 3c shows the excitation wavelength-dependent PL spectra of the cys-GQDs (0.8 wt% of L-cysteine) when excited in a range from 400 to 500 nm. The emission peaks shift from 530 nm to 545 nm and, remarkably, their intensities decrease. These results are attributed to the optical selection for the different sizes and the surface defects of GQDs, which was extensively reported with the fluorescent carbon-based nanomaterials.[22] The quantum yield of cys-GQDs (Table S1) is determined to be around 28% using quinine sulphate as a standard reference (54% in 0.5 M H_2SO_4), which is much higher than that of the pristine GQDs (8.8%). The higher quantum yield of the cys-GQDs could be attributed to L-cysteine boned on the GQDs surfaces which bears the electron-donating amine groups.[26]
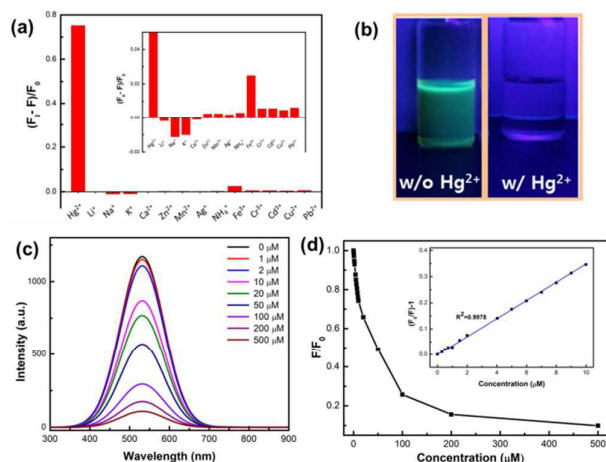
Fig. 4 (a) The fluorescence enhancement factors [$(F-F_0)/F_0$] of cys-GQDs for the various metal ions (100.0 μM). (b) The photo imgae of the cys-GQDs solutions in the presence (right) and absence of Hg^{2+} (left) under the 365nm UV light irradiation. (c) The fluorescence change of cys–GQDs with the various Hg^{2+} concentrations. (d) The dependence of F/F_0 on the concentration of Hg^{2+} in the range of 0-500 μM. The inset show a Stern-Volmer plot for the fluorescence quenching of cys–GQDs with the range of 0-10 μM.

To evaluate the fluorescent probe application, the fluorescence changes of cys-GQDs (0.8 wt% of L-cysteine) were measured in the presence of various metal ions at the same concentration of 100 μM (Fig. 4a). Due to high quantum yield

(Fig. S4) and excellent fluorescence quenching in a primary test (Fig. S5), compared to other samples, cys-GQDs with 0.8 wt% L-cysteine was chosen for the Hg^{2+} detection experiments. Impressively, whereas other metal ions exhibit negligible change of fluorescence, the addition of Hg^{2+} causes the significant fluorescence quenching of cys-GQDs to decrease by about 75%, which shows that the fluorescence quenching of cys-GQDs is highly selective for Hg^{2+}. In addition, it can be clearly observed that the green fluorescence of cys-GQDs with irradiation of 365 nm UV light quenched upon the addition of Hg^{2+} (Fig. 4b). To explore the Hg^{2+} detection sensitivity of cys-GQDs, with varying concentrations of Hg^{2+} from 1 μM to 500 μM, the fluorescence changes of cys-GQDs were measured. As shown in Fig. 4c, the fluorescence intensities gradually decreases with increasing concentrations of Hg^{2+}, and the spectral maximum peaks are retained at around 530 nm. The Hg^{2+} concentration dependent fluorescence (Fig. 4d) shows the drastic quenching from the low concentration to 100 μM, and the saturated change in the higher concentrations. The maximum fluorescence quenching of 92% is observed with an Hg^{2+} concentration of 500 μM. A Stern-Volmer plot in the range of 0-10 μM shows a linear behavior, having the correlation coefficient R^2= 0.9978 (inset of Fig. 4d). The calculated Stern-Volmer constant, K_{SV}, is found to be $3.4×10^{-7}$ M^{-1}. This value is higher than that of quenching between simple organic dyes/quencher pairs,[27] indicating efficient fluorescence quenching by the cys-GQDs and Hg^{2+} pairs. Also, the detection limit (LOM) calculated following the 3σ IUPAC criteria is 0.02 μM which is lower than that of previously reported fluorescence probes.[28-30] Furthermore, the applicability of cys-GQDs for the detection of Hg^{2+} in a real sample was examined (Fig. S6). The real river water sample was taken from Taehwa River (Ulsan city, Rep. of Korea) and the sample was first filtered by 0.22 μm membrane and centrifuged at 10,000 rpm for 20 min to remove any suspended particles. After the river water samples were prepared by adding various concentrations of Hg^{2+}, the fluorescence change of cys-GQDs was measured by the same experimental procedures. It was clearly observed that cys-GQDs show also the excellent Hg^{2+} detection performance for the real river water sample, in spite of the possible interference from mineral and organic species existing in the river water. These results demonstrate that cys-GQDs have the applicability and reliability for the practical Hg^{2+} detection in the real water.

For the fluorescence quenching mechanism of cys-GQDs in the presence of Hg^{2+}, the FT-IR spectroscopy was taken to study the chemical interaction between the cys-GQDs and Hg^{2+}. Fig. 5a presents the FT-IR spectra change of cys-GQDs upon the addition of 40 μM Hg^{2+}. The peak at 2552 cm^{-1} assigned to the S-H vibration of the thiol group of cys-GQDs almost disappears in the presence of Hg^{2+}, which may be attributed to the formation of S-Hg bonding by the deprotonation of the thiol group. Furthermore, the symmetric COO^- stretching band at 1421 cm^{-1} shifts to the lower wavelength due to the bonding interaction between Hg^{2+} and the COO^- group of cys-GQDs. These results confirm the chemical bond formation between Hg^{2+} and the cys-GQDs. The time-resolved fluorescence spectroscopy was further carried out to explore the Hg^{2+} induced

fluorescence quenching mechanism of the cys-GQDs. Fig. 5b shows the fluorescence decay of the cys-GQDs in the absence and presence of Hg^{2+} (40 µM). The fluorescence lifetime of the cys-GQDs in the absence of Hg^{2+} is found to be 7.2 ns with the excitation wavelength of 446 nm and the emission of 538 nm, indicating an excitation and recombination process of the cys-GQDs. Upon the addition of Hg^{2+} ion, the lifetime of the cys-GQDs decreases to 5.1 ns, suggesting that the dynamic fluorescent quenching occurs through a fast electron transfer between Hg^{2+} and cys-GQDs.[31,32] By the complex formation between the cys-GQDs and Hg^{2+}, the radiative recombination of excitons is constrained through an effective electron transfer process from the cys-GQD to Hg^{2+}, resulting in a remarkable fluorescence quenching as depicted in Fig. 5c.
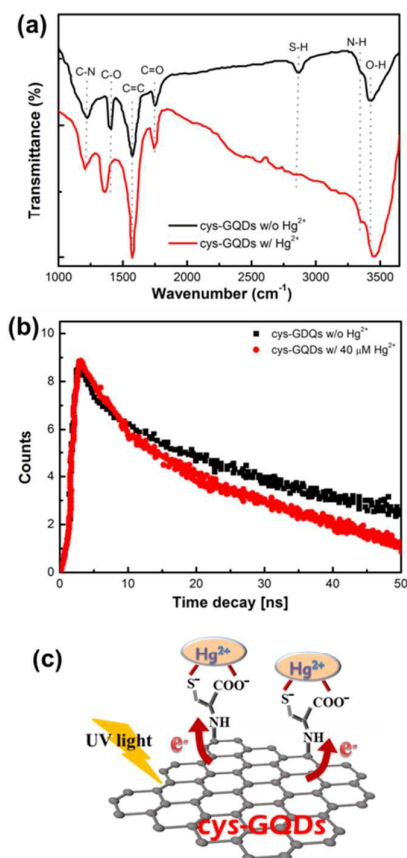
Fig. 5 (a) FT-IR spectra of cys–GQDs in the presence and absence of Hg^{2+}. (b) Fluorescence decay of cys–GQDs as the function of time in the presence of Hg^{2+}. (c) Schematic presentation of the fluorescence quenching mechanism of cys-GQDs in the presence of Hg^{2+}.

Conclusions

In conclusion, we have demonstrated the synthesis of cys-GQDs by a simple and facile process, which involves the carbonization of CA and the functionalization of L-cysteine through a hydrothermal process. The as-prepared cys-GQDs have a green fluorescence under UV irradiation and high crystallinity with uniform size distribution. It is further found that the cys-GQDs exhibit tunable fluorescence by tuning the amount of L-cysteine, which is attributed to a π-conjugated interaction between GQDs and the amine group of L-cysteine. Furthermore, the cys-GQDs show their suitability as a highly sensitive and selective fluorescent probe for Hg^{2+} detection. The significant fluorescence quenching of cys-GQDs occurs in the presence of Hg^{2+} through the electron transfer process by the complex formation complex of cys-GQDs and Hg^{2+}. Our method also has demonstrated the successful application in a real water sample. The proposed cys-GQDs were considered as environmentally friendly, low cost, and easily prepared fluorescence probes for Hg^{2+} detection, compared to tedious and complicated procedures in traditional methods. It is believed that our approach provide a low cost and facile route toward efficient fluorescent materials for sensing, bioimaging, and other applications.

Acknowledgements

References

1   K. S. Novoselov, A. K. Geim, S. V. Morozov, D. Jiang, Y. Zhang, S. V. Dubonos, I. V. Grigorieva and A. A. Firsov, *Science,* 2004, **306,** 666.
2   A. K. Geim and K. S Novoselov, *Nat. Mater.*, 2007, **6**, 183.
3   D. R. Dreyer, R. S. Ruoff and C. W. Bielawski, *Angew. Chem. Int. Ed.*, 2010, **49**, 9336.
4   Ch. K. Chua and M. Pumera, *Chem. Soc. Rev.*, 2013, **42**, 3222.
5   L. A. Ponomarenko, F. Schedin, M. I. Katsnelson, R. Yang, E.W. Hill, K. S. Novoselov and A. K. Geim, *Science*, 2008, **320**, 356.
6   L. Li, G. Wu, G. Yang, J. Peng, J. Zhao and J.-J. Zhu, *Nanoscale*, 2013, **5,** 4015.
7   S. H. Jin, D. H. Kim, G. H. Jun, S. H. Hong and S. Jeon, *ACS Nano,* 2013, **7**, 1239.
8   H. Tao, K. Yang, Z .Ma, J. Wan, Y. Zhang, Z. Kang and Z. Liu, *Small*, 2012, **8**, 281.
9   J. Peng, W. Gao, B. K. Gupta. Z. Liu, R. Romero-Aburto, L. Ge, L. Song, L. B. Alemany, X. Zhan, G. Gao, S. A. Vithayathil, B. A. Kaipparettu, A. A. Marti, T. Hayashi, J. J. Zhu and P. M. Ajayan, *Nano Lett.*, 2012, **12**, 844.
10   L. L. Li, J. Ji, R. Fei, C. Z. Wang, Q. Lu, J. R. Zhang, L. P. Jiang abd J. J. Zhu, *Adv. Funct. Mater.,* 2012, **22**, 2917.
11   D. Y. Pan, J. C. Zhang, Z. Li and M. H. Wu, *Adv. Mater.*, 2010, **22**, 734.
12   K. Habiba, V. I. Makarov, J. Avalos, M. J. F. Guinel, B. R. Weiner and G. Morell, *Carbon*, 2013, **64**, 341.
13   J. Shen, Yi. Z. X. Yang and C. Li, *Chem. Commu.*, **2012**, 48, 3686.
14   C. K. Chua and M. Pumera, *Chem. Soc. Rev.*, 2014, **43**, 291.
15   R. Sekiya, Y. Uemura, H. Murakami and T. Haino, *Angew. Chem. Int. Ed.*, 2014, **126**, 5725.
16   A. A. Nahain, J. E. Lee, I. In, H. Lee, K. D. Lee, J. H. Jeong and S. Y. Park, *Mol. Pharmaceutics*, 2013 10, 3736.
17   Y. Chen and Z. Rosenzweig, *Anal. Chem.*, 2002, **74**, 5132.

18 A. M. Derfus, W. C. W. Chan and S. N. Bhatia, *Nano Lett*., 2004, **4**, 11.

19 H. Sun, L. Wu, W. Wei and X. Qu, *Mater. Today,* 2013, **16**, 433.

20 T. V. Tam, N. B. Trung, H. R. Kim, J. S. Chung and W. M. Choi, *Sens. Actua. B*, 2014, **202**, 568.

21 S. Muralikrishna, K. Sureshkumar, Thomas S. Varley, D. H. Nagaraju and T. Ramakrishnappa, *Anal. Methods,* 2014, 6, 8698.

22 S. Zhu, J. Zhang, Ch. Qiao, S. Tang, Y. Li, W. Yuan, B. Li, L. Tian, F. Liu, R. Hu, H. Gao, H. Wei, H. Zhang, H. Ch. Sun and B. Yang, *Chem. Commu.,* 2011, **47**, 6858.

23 V. Georgakilas, M. Otyepka, A. B. Bourlinos, V. Chandra, N. Kim, K. C. Kemp, P. Hobza, R. Zboril and K. S. Kim, *Chem. Rev*., 2012, **112**, 6156.

24 N. H. Kim, T. Kuila and J. H. Lee, *J. Mater. Chem. A*, 2014, **2**, 2681.

25 Y. Lu, Y. Jiang, W. Wei, H. Wu, M. Liu, L. Niu and W. Chen, *J. Mater. Chem*., 2012, **22,** 2929.

26 H. Tetsuka, R. Asahi, A. Nagoya, K. Okamoto, I. Tajima, R.Ohta and A. Okamoto, *Adv. Mater.*, 2012, **24,** 5333.

27 J. R. Lakowicz, Principle of fluorescence spectroscopy, 3rd ed, 1999.

28 K. Zhang, Y. Yu and S. Sun, *Appl. Surf. Sci*., 2013, **276**, 333.

29 R. Zhang and W. Chen, *Biosens. Bioelectron*., 2014, **55**, 83.

30 L. Li, G. Wu, T. Hong, Z. Yin, D. Sun, E. S. Abdel-Halim and J. Zhu, *ACS Appl. Mater. Interfaces*, 2014, **6**, 2858.

31 Q. Lu, Y. Zhang and S. Lui, *J. Mater. Chem. A.,* 2015, **3**, 8552.

32 Q. Lu, W. Wei, Z. Zhou, Z. Zhou, Y. Zhang and S. Liu, *Analyst*, 2014, **139**, 2404.

Facile synthesis of cysteine-functionalized graphene quantum dots

for a fluorescence probe for mercury ions

Tran Van Tam, Soon Ho Hong*, Won Mook Choi*

School of Chemical Engineering, University of Ulsan, 93 Daehak-ro Nam-gu, Ulsan 680-749, Republic of Korea.

We synthesized cystenine-functionalized graphene quantum dots (cys-GQDs) by a simple, low cost and environmentally friendly method and demonstrated as highly sensitive and selective fluorescence probes for Hg^{2+} detection.